

Improved carbon dioxide absorption in double-charged ionic liquids

Jocasta Avila,[†] Luiz Fernando Lepre,[†] Kateryna Goloviznina,[†] Lorenzo Guazzelli,[‡] Christian Silvio Pomeli,[‡] Cinzia Chiappe,[‡] Agilio Pádua,[†] and Margarida Costa Gomes^{*,†}

[†]*Laboratoire de Chimie de l'ENS Lyon, CNRS and Université de Lyon, 46 allée d'Italie,
69364 Lyon, France*

[‡]*Department of Pharmacy, University of Pisa, Via Bonanno 33, 56126 Pisa, Italy*

E-mail: margarida.costa-gomes@ens-lyon.fr

Supplementary Information

Ionic liquid mixtures

Table S1: Sample nomenclature and composition of the ionic liquids and of the ionic liquid mixtures.

Sample	Chemicals	m_{IL1} (g)	m_{IL2} (g)	$\chi(2)$
IL1	[tetraEG(mim) ₂][OAc] ₂	-	-	-
$\chi_2 = 0.25$	([tetraEG(mim) ₂][OAc] ₂) _{0.75} ([C ₂ mim][OAc]) _{0.25}	1.57660	0.20240	0.2502
$\chi_2 = 0.50$	([tetraEG(mim) ₂][OAc] ₂) _{0.50} ([C ₂ mim][OAc]) _{0.50}	1.23670	0.53570	0.5297
$\chi_2 = 0.75$	([tetraEG(mim) ₂][OAc] ₂) _{0.25} ([C ₂ mim][OAc]) _{0.75}	0.75220	0.92200	0.7611
IL2	[C ₂ mim][OAc]	-	-	-

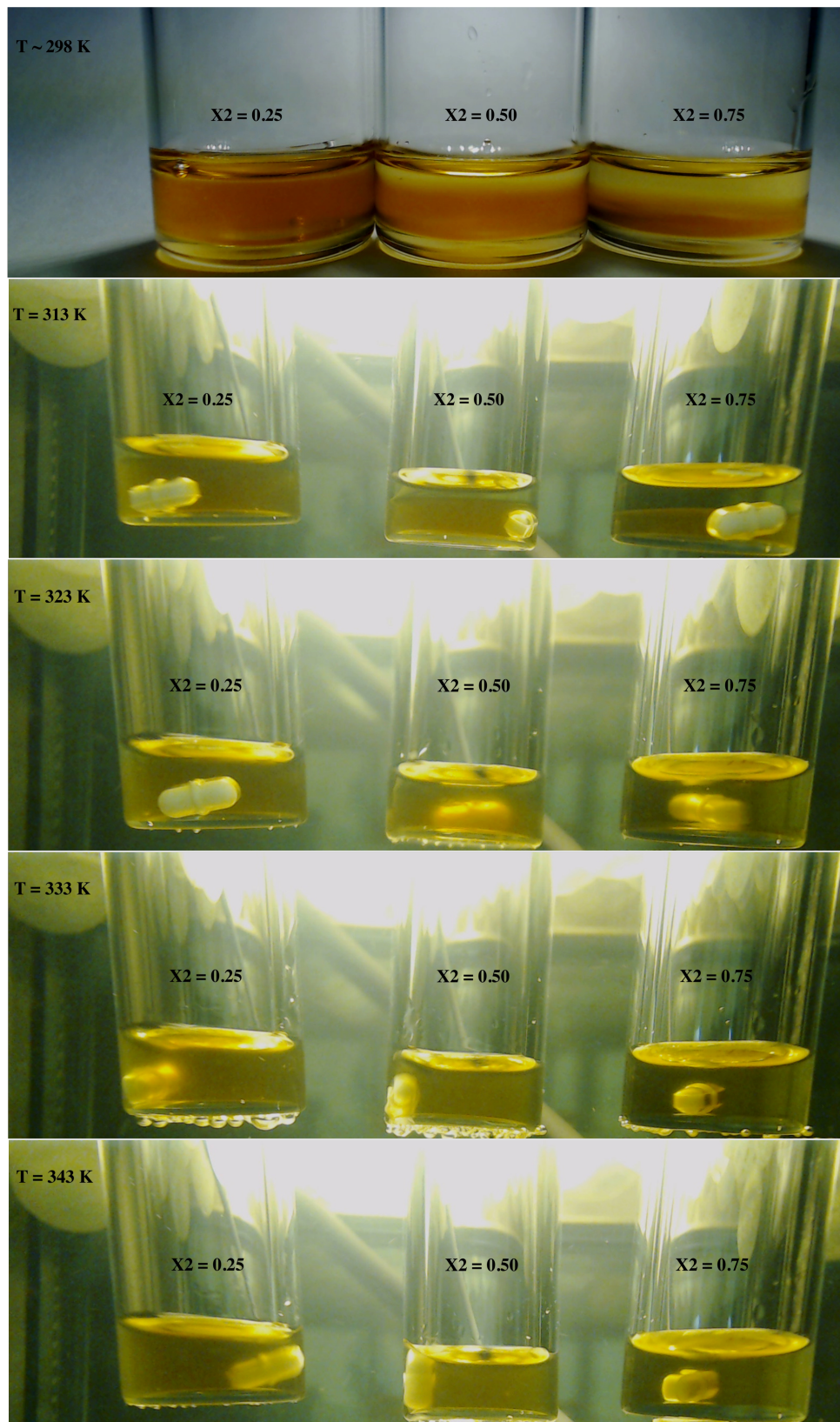


Figure S1: $([\text{tetraEG}(\text{mim})_2][\text{OAc}]_2)_{\chi_1} + ([\text{C}_2\text{mim}][\text{OAc}])_{\chi_2}$ mixtures with compositions $\chi_2 = 0.25$, $\chi_2 = 0.50$ and $\chi_2 = 0.75$, at different temperatures. At 298 K two liquid phases are visible. Above 313 K the ILs are fully miscible.

Sorption balance measurements

Gas absorption in ionic liquids was measured using an IGA 001 gravimetric microbalance, whose working principle is represented in Figure S2, with instrument conditions and parameters listed in Table S2.

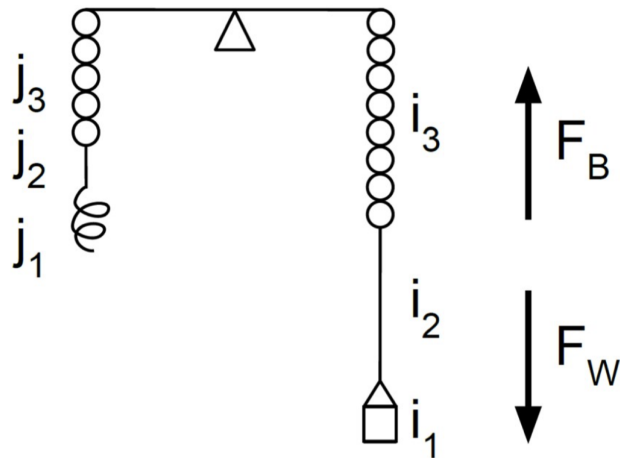


Figure S2: Schematic diagram of the IGA 001 gravimetric microbalance. The symbols i and j , described in Table S2, represent the components on the sample side and on the counterweight side of the microbalance, respectively. F_W and F_B are the forces experienced on the sample side of the microbalance with the arrows indicating the direction of these forces: the weight due to gravity (F_W) and the buoyancy due displacement of gas (F_B).^{1?}

Table S2: IGA 001 microbalance components and working parameters.

Subscript	Item	Mass/g	Material	Density /g cm ⁻³	T /K
s	degassed sample	m_s	Described in Table 1	ρ_s	T_s
a	adsorbed gas	m_g	CO ₂		T_s
i_1	sample container	0.6032	stainless steel	7.9	T_s
i_2	wire	0.0644	tungsten	21.0	T_s
i_3	chain	0.1934	gold	19.8	318
j_1	counterweight	0.7870	stainless steel	7.9	308
j_2	hook	0.0054	tungsten	21.0	308
j_3	chain	0.1498	gold	19.8	318

Density and molar volume data

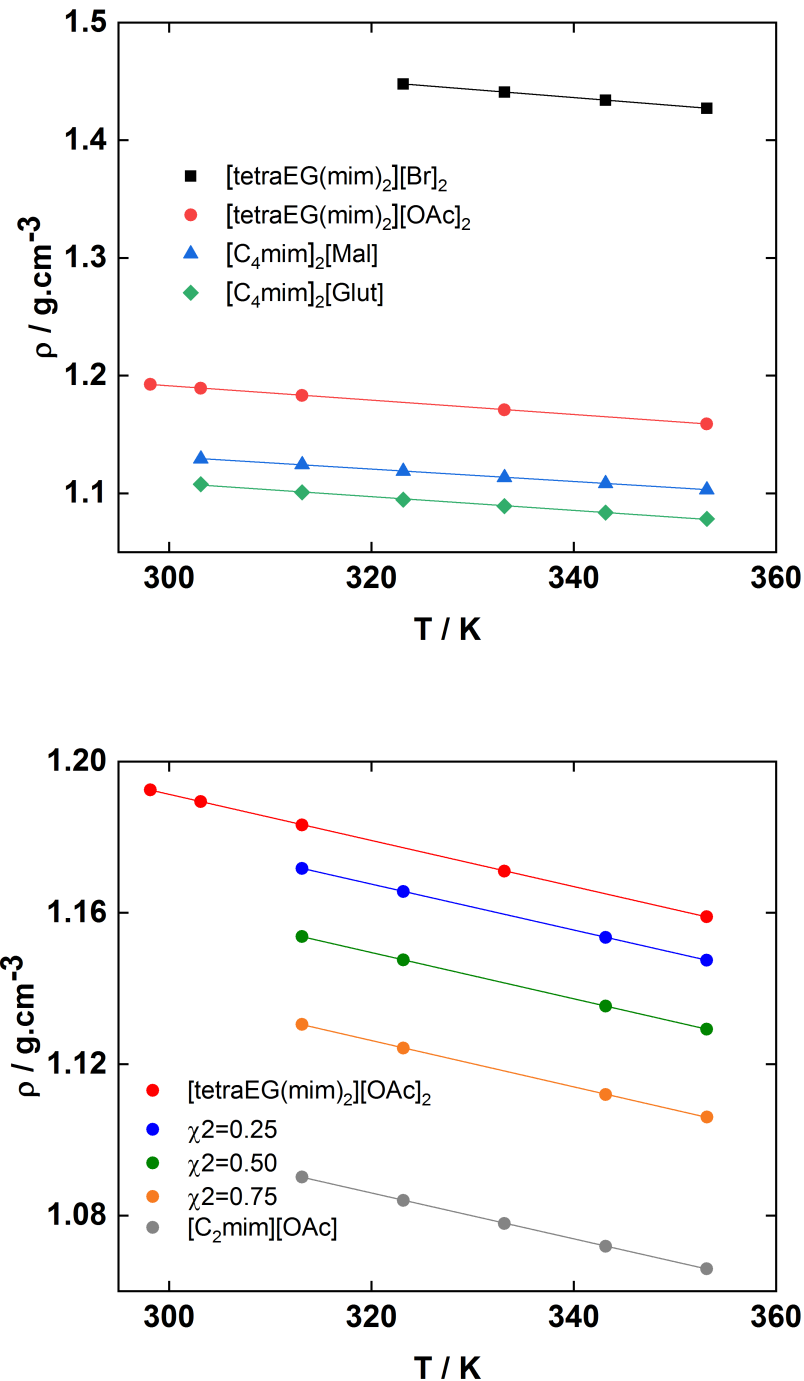


Figure S3: Experimental densities (symbols) of the (Top) [tetraEG(mim)₂][Br]₂, [tetraEG(mim)₂][OAc]₂, [C₄mim]₂[Mal], [C₄mim]₂[Glut] and (Bottom) [tetraEG(mim)₂][OAc]₂, ([tetraEG(mim)₂][OAc]₂) _{χ_1} + ([C₂mim][OAc]) _{χ_2}) mixtures and [C₂mim][OAc] as a function of the temperature, expressed as linear functions (solid lines).

Table S3: Experimental densities of $[\text{tetraEG}(\text{mim})_2][\text{OAc}]_2$, $([\text{tetraEG}(\text{mim})_2][\text{OAc}]_2)_{\chi 1} + ([\text{C}_2\text{mim}][\text{OAc}])_{\chi 2}$ mixtures and $[\text{C}_2\text{mim}][\text{OAc}]$ as a function of the temperature. The deviations indicated are relative to the fitting polynomials with coefficients listed in Table S4

T/K	$\rho/\text{g cm}^{-3}$	$\delta/\%$	T/K	$\rho/\text{g cm}^{-3}$	$\delta/\%$
$[\text{tetraEG}(\text{mim})_2][\text{OAc}]_2$					
298.151	1.192528	-0.007	313.149	1.171757	-0.002
303.148	1.189406	-0.0009	323.149	1.165649	0.002
313.149	1.183211	0.007	343.149	1.153532	0.0006
333.149	1.171015	0.008	353.149	1.147483	-0.0009
353.149	1.158992	-0.007			
$\chi_2 = 0.25$					
313.149	1.153702	-0.002	313.149	1.130489	-0.004
323.149	1.147558	0.001	323.149	1.124275	0.004
343.149	1.135319	0.003	343.149	1.112008	0.005
353.149	1.129264	-0.002	353.149	1.105998	-0.005
$\chi_2 = 0.50$					
313.149	1.153702	-0.002	313.149	1.130489	-0.004
323.149	1.147558	0.001	323.149	1.124275	0.004
343.149	1.135319	0.003	343.149	1.112008	0.005
353.149	1.129264	-0.002	353.149	1.105998	-0.005
$[\text{C}_2\text{mim}][\text{OAc}]$					
313.150	1.090181	-0.005			
323.150	1.084017	0.002			
333.150	1.077926	0.005			
343.150	1.071897	0.002			
353.150	1.065925	-0.005			

Table S4: Parameters A_0 and A_1 from linear functions used to fit the experimental densities, $\rho = A_0 + A_1 T$, as a function of temperature and absolute average deviation (AAD)

Sample	$A_0/\text{g cm}^{-3}$	$A_1/\text{g cm}^{-3} \text{ K}^{-1}$	$\text{AAD}/\%$
$[\text{tetraEG}(\text{mim})_2][\text{Br}]_2$	1.6696	-6.8971×10^{-4}	0.003
$[\text{tetraEG}(\text{mim})_2][\text{OAc}]_2$	1.3742	-6.0965×10^{-4}	0.006
$[\text{C}_4\text{mim}]_2[\text{Mal}]$	1.2891	-5.2683×10^{-4}	0.01
$[\text{C}_4\text{mim}]_2[\text{Glut}]$	1.2838	-5.8346×10^{-4}	0.04
$\chi_2 = 0.25$	1.3617	-6.0664×10^{-4}	0.001
$\chi_2 = 0.50$	1.3451	-6.1115×10^{-4}	0.002
$\chi_2 = 0.75$	1.3222	-6.1249×10^{-4}	0.005
$[\text{C}_2\text{mim}][\text{OAc}]$	1.2781	-6.0144×10^{-4}	0.004

Table S5: Parameters B_0 and B_1 from linear functions used to fit the molar volume, $V_m = B_0 + B_1 T$, as a function of temperature and absolute average deviation (AAD)

Sample	$B_0/\text{cm}^3 \text{ mol}^{-1}$	$B_1/\text{cm}^3 \text{ mol}^{-1} \text{ K}^{-1}$	AAD/%
[tetraEG(mim) ₂][Br] ₂	282.46	0.1609	0.0003
[tetraEG(mim) ₂][OAc] ₂	312.87	0.1952	0.001
[C ₄ mim] ₂ [Mal]	288.07	0.1609	0.01
[C ₄ mim] ₂ [Glut]	308.50	0.1996	0.003
[C ₂ mim][OAc]	128.32	0.08881	0.0004

Table S6: Number of groups (n_j) taken into account for the calculation of the molar volume of the studied ILs using the group contribution method expressed by Eq. 4 (main text).

Group j	n_j	
	[tetraEG(mim) ₂][Br] ₂	[tetraEG(mim) ₂][OAc] ₂
-O ⁻	3	3
-CH ₂ ⁻	8	8
[C ₀ ImC ₁] ₂ ²⁺	1	1
Br	2	0
CH ₃ COO ⁻	0	2
	[C ₄ mim] ₂ [Mal]	[C ₄ mim] ₂ [Glut]
[C ₄ ImC ₁] ⁺	2	2
-COO ⁻	2	2
-CH ₂ ⁻	1	3
	[C ₂ mim][OAc]	
[C ₂ ImC ₁] ⁺	1	
[CH ₃ COO] ⁻	1	

Table S7: Group contribution parameters used to calculate the molar volume using Eq. 4 (main text).

Group j	$\frac{C_0}{\text{cm}^3 \text{mol}^{-1}}$	$\frac{C_1}{\text{cm}^3 \text{mol}^{-1} \text{K}^{-1}}$	$\frac{C_2}{\text{cm}^3 \text{mol}^{-1} \text{K}^{-2}}$	Ref.
$-\text{O}^-$	4.571	1.869×10^{-3}	2.058×10^{-5}	2
$-\text{CH}_2^-$	16.967	1.399×10^{-3}	-1.946×10^{-6}	2
$[\text{C}_2\text{ImC}_1]^+$	100.017	6.955×10^{-2}	2.996×10^{-5}	3
$[\text{C}_4\text{ImC}_1]^+$	134.260	8.890×10^{-1}	4.304×10^{-5}	3
$[(\text{C}_0\text{ImC}_1)_2]^{2+}$	106.336	1.482×10^{-1}	-7.549×10^{-5}	4
Br	27.120			3
$-\text{COO}^-$	21.68	3.101×10^{-2}	-4.332×10^{-4}	2
CH_3COO^-	49.177	2.149×10^{-2}	-2.775×10^{-5}	3

Viscosity data

Table S8: Experimental viscosities of the $[\text{tetraEG}(\text{mim})_2][\text{OAc}]_2$, $([\text{tetraEG}(\text{mim})_2][\text{OAc}]_2)_{\chi 1} + ([\text{C}_2\text{mim}][\text{OAc}])_{\chi 2}$ mixtures and $[\text{C}_2\text{mim}][\text{OAc}]$ as a function of the temperature. The deviations indicated are relative to the Vogel-Tammann-Fulcher (VTF) functions with coefficients listed in Table S9

T/K	$\eta/\text{m Pas}$	$\delta/\%$	T/K	$\eta/\text{m Pas}$	$\delta/\%$
$[\text{tetraEG}(\text{mim})_2][\text{OAc}]_2$					
323.151	2251.9	0.01	328.151	526.38	0.002
333.149	971.44	-0.02	333.149	372.29	-0.01
343.149	478.01	0.1	343.149	202.01	0.003
353.149	262.15	-0.2	353.149	119.99	-0.002
$\chi_2 = 0.25$					
323.151	377.54	0.0006	313.149	284.06	0.002
333.150	197.56	-0.008	323.150	149.06	-0.03
343.150	114.54	0.03	333.150	86.989	0.09
353.150	72.025	-0.03	343.150	55.303	-0.08
			353.151	37.426	-0.005
$\chi_2 = 0.50$					
323.151	377.54	0.0006	313.149	284.06	0.002
333.150	197.56	-0.008	323.150	149.06	-0.03
343.150	114.54	0.03	333.150	86.989	0.09
353.150	72.025	-0.03	343.150	55.303	-0.08
			353.151	37.426	-0.005
$\chi_2 = 0.75$					
$[\text{C}_2\text{mim}][\text{OAc}]$					
313.150	54.620	0.01			
323.150	35.067	-0.08			
333.150	24.068	0.2			
343.150	17.549	-0.09			
353.150	13.323	-0.05			

Table S9: Parameters A , B and T_0 from VTF functions used to fit the experimental viscosity, $\eta = Ae^{(B/(T-T_0))}$, as a function of temperature and the corresponding absolute average deviation (AAD)

Sample	A/mPas	B/K	T_0/K	$AAD/\%$
[tetraEG(mim) ₂][Br] ₂	2.6606×10^{-8}	7137.52	78.40	13
[tetraEG(mim) ₂][OAc] ₂	0.1296	1035.75	216.91	0.08
[C ₄ mim] ₂ [Mal]	5.0387×10^{-8}	6336.71	87.15	17
[C ₄ mim] ₂ [Glut]	4.5584×10^{-3}	2173.40	160.61	2
$\chi_2 = 0.25$	0.1644	899.51	216.71	0.02
$\chi_2 = 0.50$	0.2095	792.67	217.42	0.02
$\chi_2 = 0.75$	0.2373	707.84	213.28	0.02
[C ₂ mim][OAc]	0.3156	546.57	207.10	0.08

Gas absorption data

Table S10: Absorption and desorption of CO₂ by [tetraEG(mim)₂][Br]₂, [tetraEG(mim)₂][OAc]₂, [C₄mim]₂[Mal] and [C₄mim]₂[Glut] as function of pressure from 0.25–5 bar at 343 K.

T/K	p/bar	χ_{CO_2}	T/K	p/bar	χ_{CO_2}
CO ₂ — Absorption					
[tetraEG(mim) ₂][Br] ₂			[tetraEG(mim) ₂][OAc] ₂		
343.265	0.0000	0.0000	343.019	0.0000	0.0000
343.096	0.2482	0.0064	343.115	0.4953	0.2375
343.106	0.4987	0.0106	343.130	0.7457	0.2975
343.101	0.7492	0.0140	343.082	0.9962	0.3221
343.110	0.9944	0.0210	343.086	1.9989	0.3669
343.168	1.9928	0.0450	343.130	2.9909	0.3924
343.149	2.9990	0.0645	343.130	3.9956	0.4108
343.135	3.9872	0.0829	343.082	4.9829	0.4255
343.139	4.9916	0.1014			
[C ₄ mim] ₂ [Mal]			[C ₄ mim] ₂ [Glut]		
339.907	0.0000	0.0000	343.907	0.0000	0.0000
343.106	0.2481	0.1301	343.106	0.2481	0.1619
343.101	0.4986	0.1960	343.101	0.4986	0.2394
343.101	0.7488	0.2407	343.101	0.7488	0.2905
343.091	0.9986	0.2715	343.091	0.9986	0.3250
343.101	1.9987	0.3209	343.101	1.9987	0.3791
343.101	2.9993	0.3457	343.101	2.9993	0.4058
343.115	3.9986	0.3577	343.115	3.9986	0.4187
343.106	4.9971	0.3667	343.106	4.9971	0.4282
CO ₂ — Desorption					
[tetraEG(mim) ₂][Br] ₂			[tetraEG(mim) ₂][Br] ₂		
343.139	4.9916	0.1014	343.082	4.9829	0.4255
343.072	3.9949	0.0840	343.125	3.9955	0.4116
343.110	2.9993	0.0659	343.082	2.9871	0.3935
343.067	1.9918	0.0479	343.125	1.9831	0.3700
343.091	0.9950	0.0239	343.106	0.9914	0.3324
343.115	0.7485	0.0168	343.096	0.7449	0.3125
343.120	0.4989	0.0126	343.125	0.4972	0.2907
343.096	0.2481	0.0087	343.110	0.2426	0.2586
343.139	0.0000	0.0000	343.019	0.0000	0.0000
[C ₄ mim] ₂ [Mal]			[C ₄ mim] ₂ [Glut]		
343.106	4.9971	0.3667	343.106	4.9971	0.4283
343.120	3.9977	0.3481	343.120	3.9977	0.4084
343.115	2.9987	0.3272	343.115	2.9987	0.3860
343.101	1.9991	0.2996	343.101	1.9991	0.3560
343.110	0.9993	0.2567	343.110	0.9994	0.3085
343.101	0.7492	0.2354	343.101	0.7492	0.2846
343.120	0.4988	0.2101	343.120	0.4988	0.2557

T/K	p/bar	χ_{CO_2}	T/K	p/bar	χ_{CO_2}
343.106	0.2492	0.1728	343.106	0.2492	0.2124
340.692	0.0000	0.0000	340.692	0.0000	0.0000

MD data

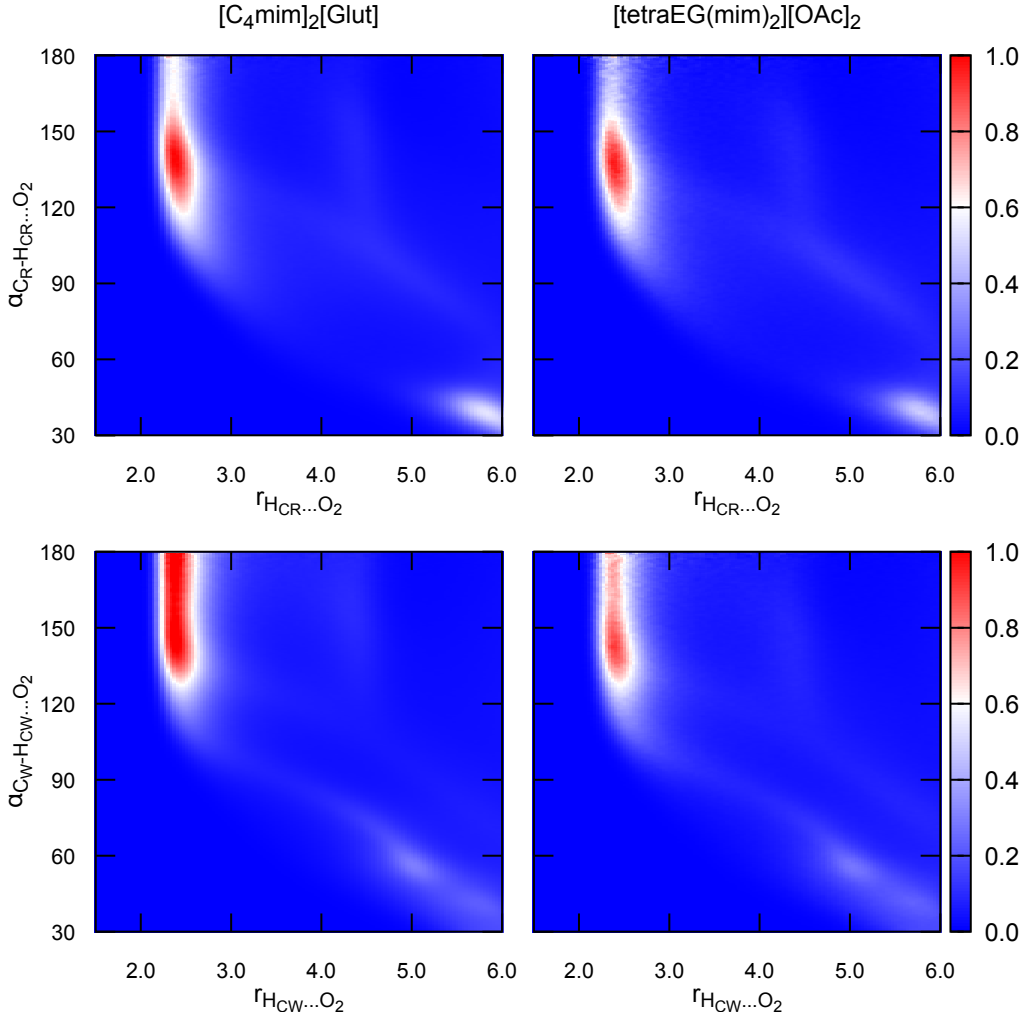


Figure S4: Probability contours revealing intermolecular hydrogen bonds in $[\text{C}_4\text{mim}]_2[\text{Glut}]$ (left) and $[\text{tetraEG}(\text{mim})_2][\text{OAc}]_2$ (right). The x -axis represent the distances between the H atoms of the imidazolium ring and O atoms of the anion. The y -axis represent the angles formed by the C–H \cdots O hydrogen bonds, where C is a carbon atom attached to the hydrogen. The color bar associated with the probability of interaction is identical across the plots.

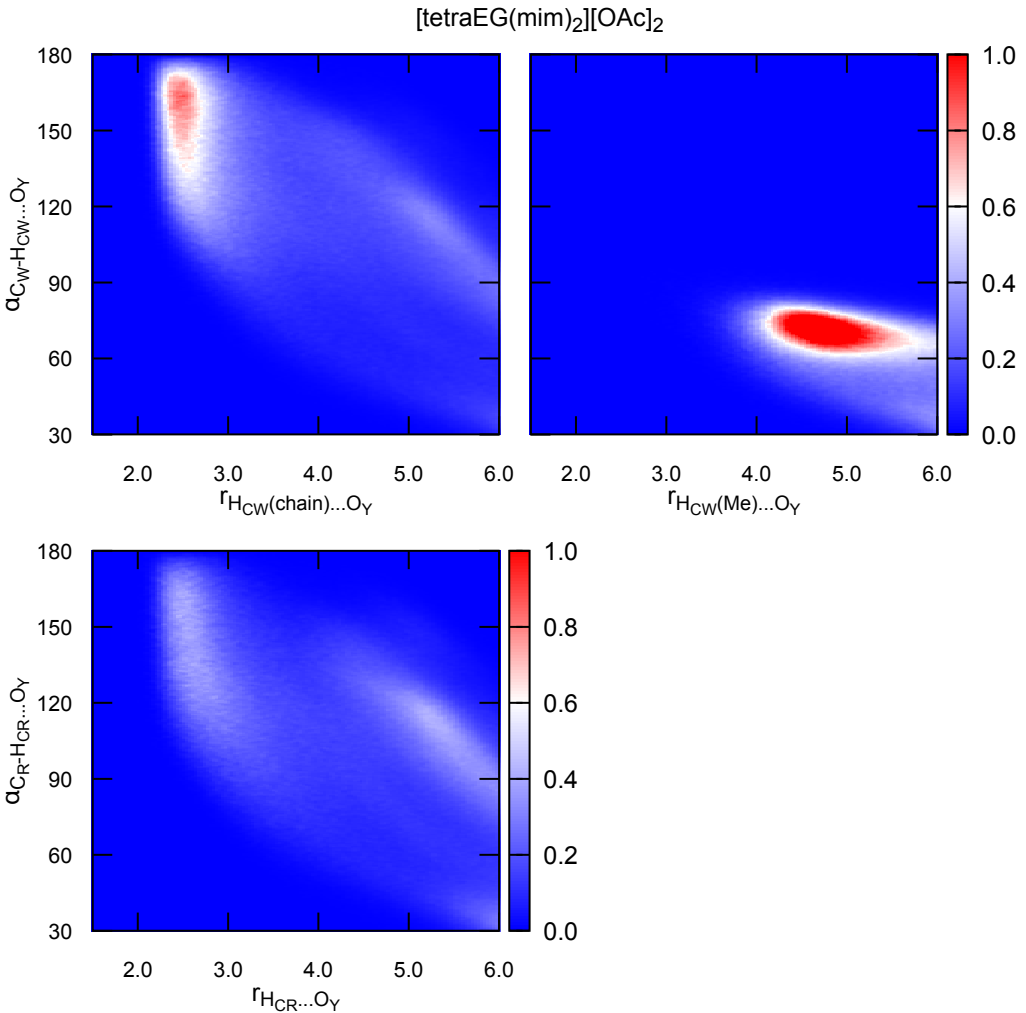


Figure S5: Probability contours revealing intramolecular hydrogen bonds in the $[\text{tetraEG}(\text{mim})_2]^{2+}$ cation. The x -axes represent the distances between the H atoms of the imidazolium ring and central O atoms of the ether side chain. The y -axes represent the angles formed by the C–H \cdots O hydrogen bonds, where C is a carbon atom attached to the hydrogen. The non-equivalent H_{cw} (chain) and H_{cw} (Me) are the H_{cw} atoms of the imidazolium ring closest to the ether side chain or to the N-methyl group, respectively. The color bar associated with the probability of interaction is identical across the plots and coincides with the color bar of Fig. S4.

NMR data

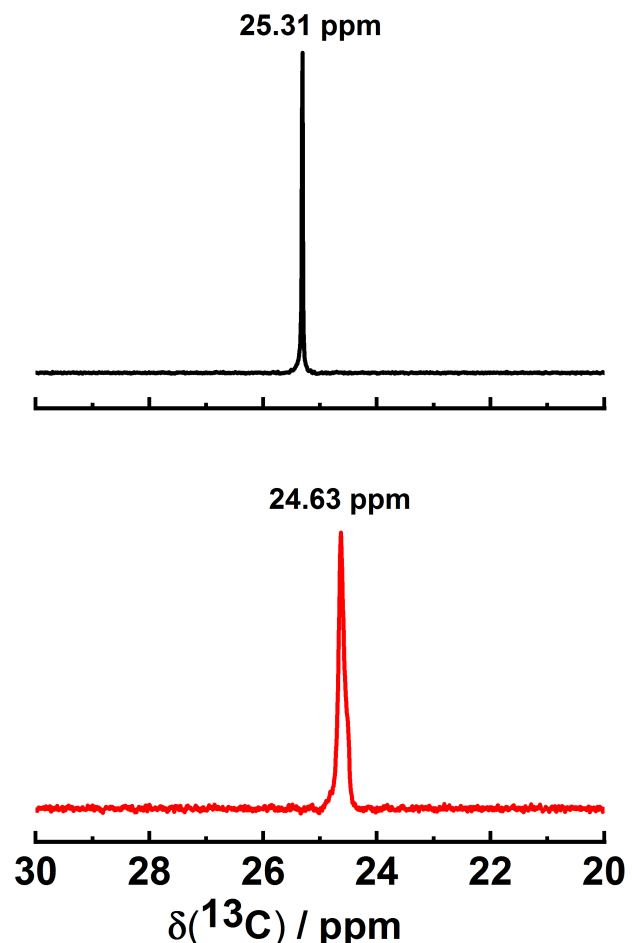


Figure S6: ^{13}C NMR spectra of $[\text{tetraEG}(\text{mim})_2][\text{OAc}]_2$ at 343 K under vacuum (top, black line) and at 10 bar of CO_2 (bottom, red line).

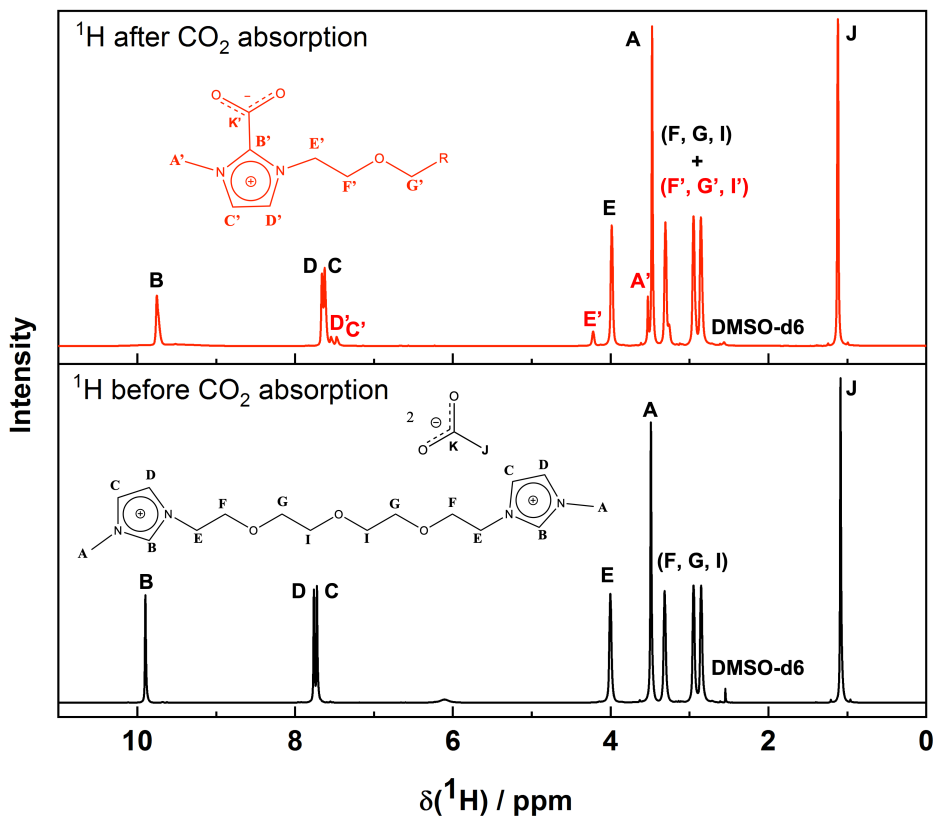


Figure S7: ^1H NMR spectra of $[\text{tetraEG}(\text{mim})_2][\text{OAc}]_2$ at 343 K under vacuum (bottom, black line) and at 10 bar of CO_2 (top, red line). The NMR peaks were assigned according to Jadhav *et al.*,⁵ Lepre *et al.*,¹ and Besnard *et al.*⁶

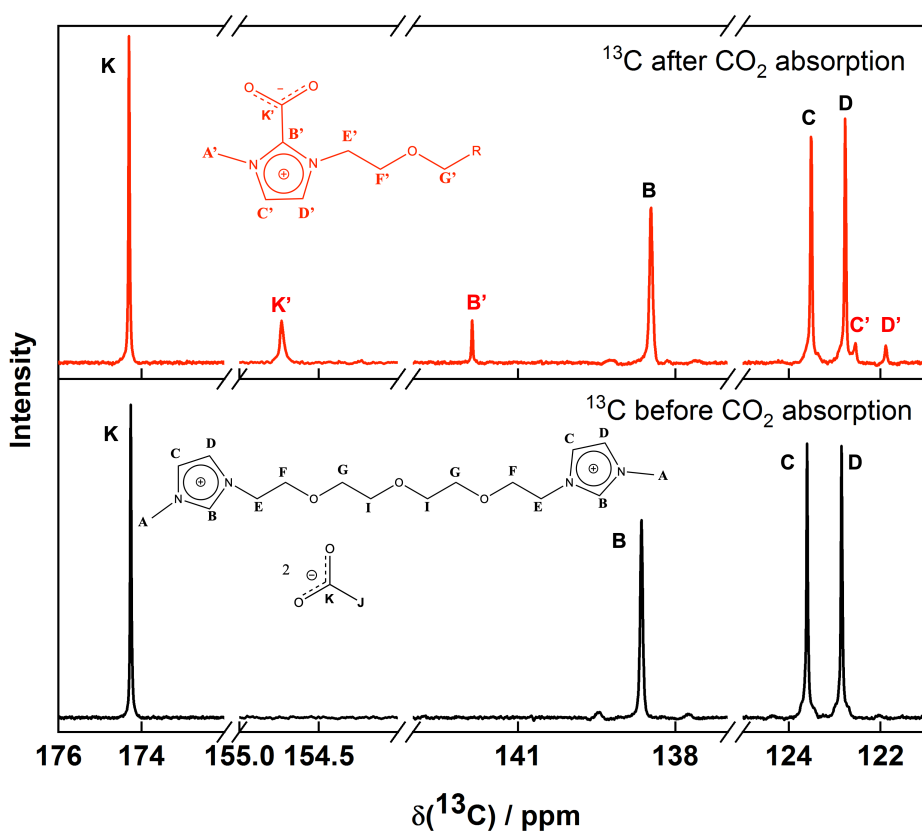
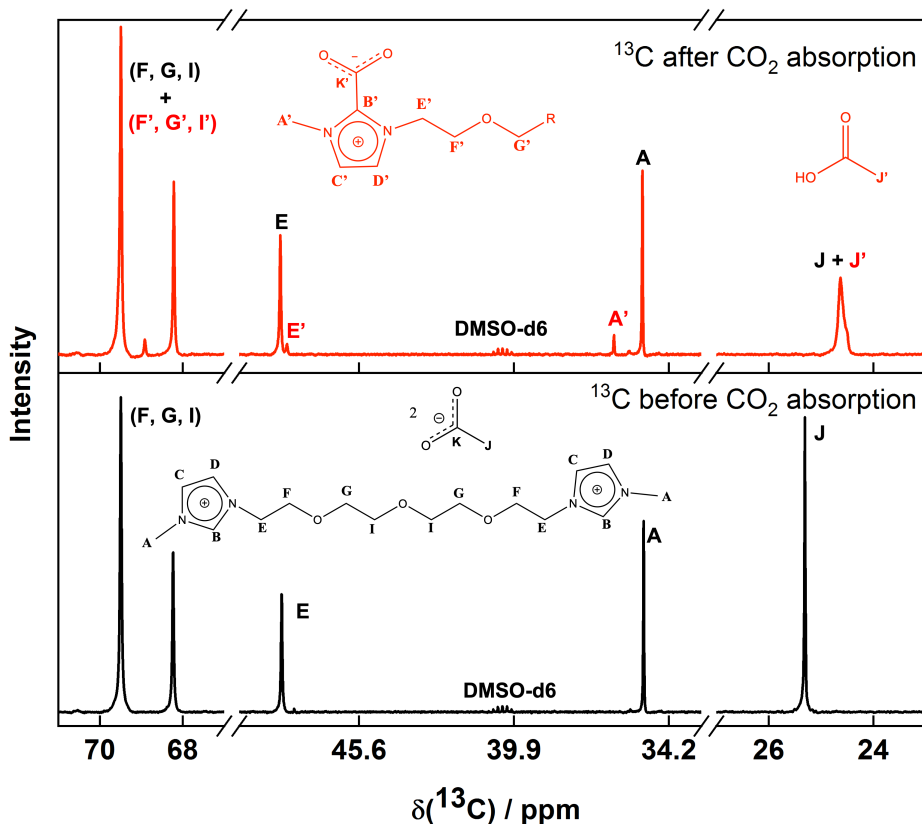


Figure S8: ^{13}C NMR spectra of $[\text{tetraEG}(\text{mim})_2][\text{OAc}]_2$ at 343 K under vacuum (bottom, black line) and at 10 bar of CO_2 (top, red line). The NMR peaks were assigned according to Jadhav *et al.*,⁵ Lepre *et al.*,¹ and Besnard *et al.*⁶

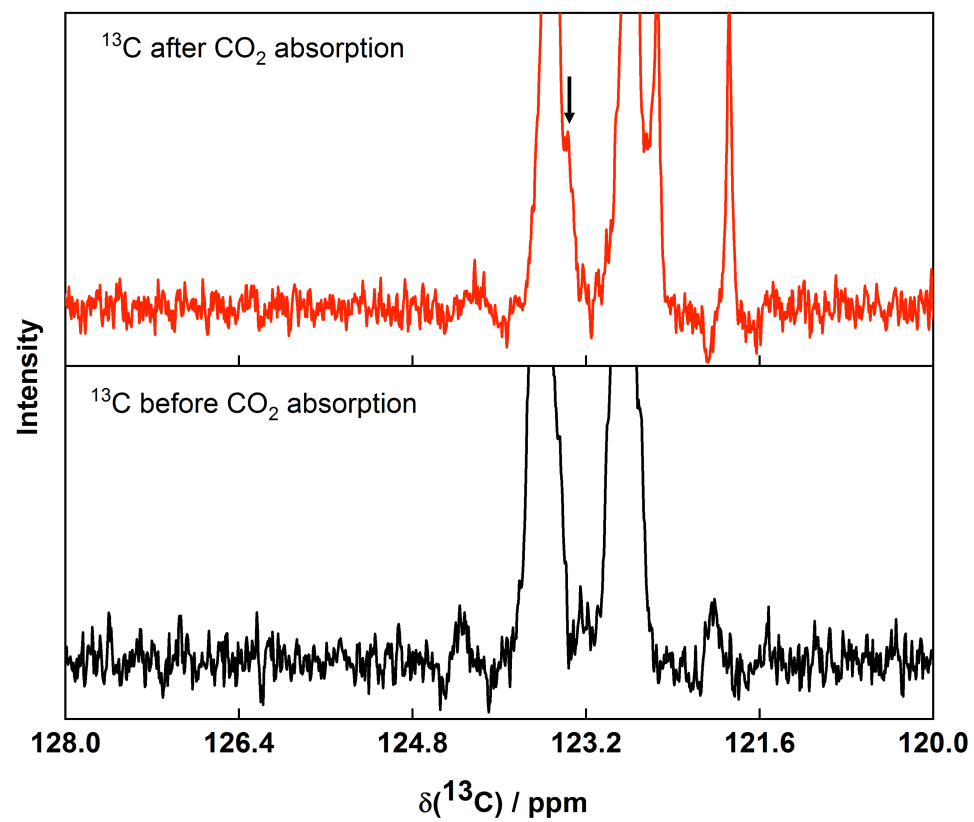


Figure S9: ^{13}C NMR spectra of $[\text{tetraEG}(\text{mim})_2][\text{OAc}]_2$ at 343 K under vacuum (bottom, black line) and at 10 bar of CO_2 (top, red line). The arrow highlights a new peak at *ca.* 123.4 ppm, which might corresponds to the CO_2 in solution.

Calculation of equilibrium constants

Once the species involved in the CO₂ absorption are identified and the amount of gas absorbed is determined, the chemical and physical contributions of the total absorption can be determined. The procedure described in our previous work was followed to calculate the equilibrium constant and the Henry's law constant for the three ionic liquids at 343 K. As indicated in Figure S10, we have considered that the reaction between CO₂ and the ionic liquid followed a 1:2 stoichiometry (blue lines)¹ or a 1:1 stoichiometry (red lines).⁷ The results show that the reaction between CO₂ and the ionic liquids follows preferentially a 1:1 stoichiometry.

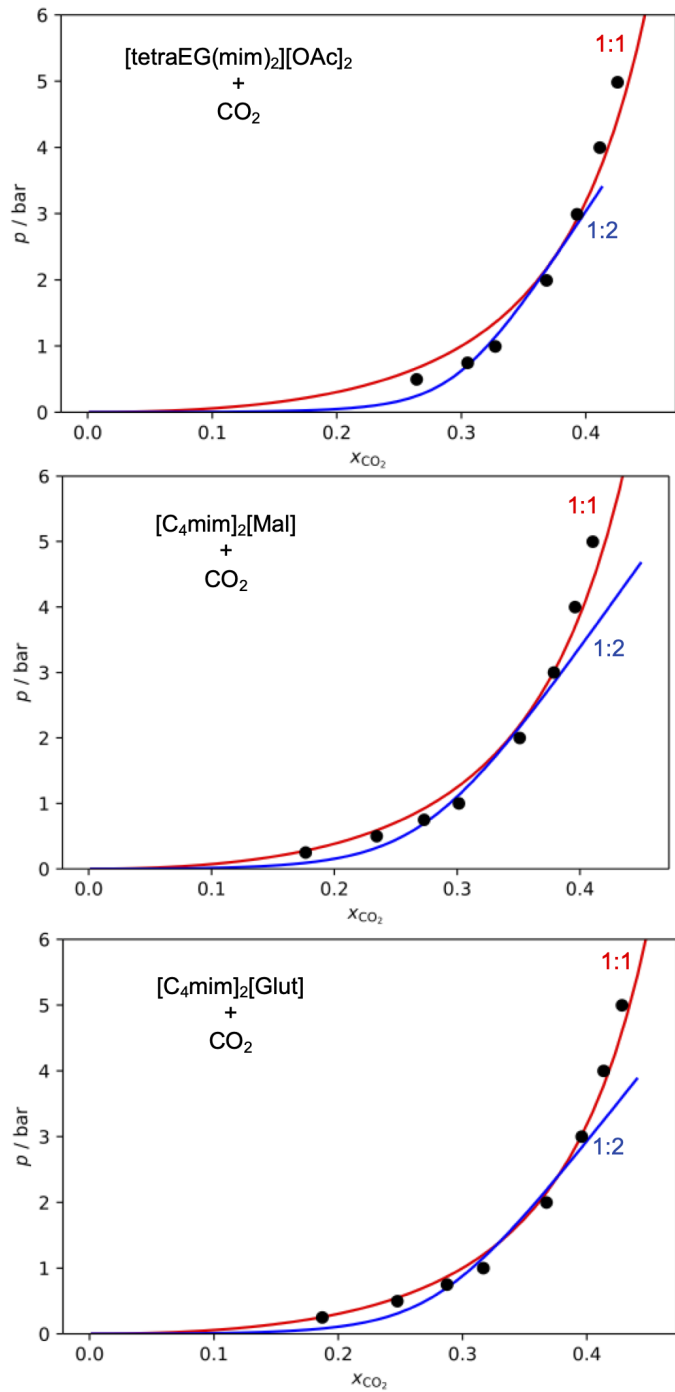


Figure S10: Fit of the gas absorption data to calculate Henry's law constant and the equilibrium constant of the reaction of carbon dioxide with the ionic liquids. The blue lines correspond to the fit considering a 1:2 stoichiometry of the reaction ¹ and the red lines concern the fit of the data assuming a 1:1 stoichiometry ⁷ of the chemical reaction of CO_2 with the ionic liquids.

References

- (1) Lepre, L. F.; Szala-Bilnik, J.; Pison, L.; Traïkia, M.; Pádua, A. A.; Ando, R. A.; Costa Gomes, M. F. Can the tricyanomethanide anion improve CO₂ absorption by acetate-based ionic liquids? *Phys. Chem. Chem. Phys.* **2017**, *19*, 12431–12440.
- (2) Deng, Y.; Morrissey, S.; Gathergood, N.; Delort, A. M.; Husson, P.; Costa Gomes, M. F. The presence of functional groups key for biodegradation in ionic liquids: Effect on gas solubility. *ChemSusChem* **2010**, *3*, 377–385.
- (3) Jacquemin, J.; Ge, R.; Nancarrow, P.; Rooney, D. W.; Costa Gomes, M. F.; Pádua, A. A.; Hardacre, C. Prediction of ionic liquid properties. I. Volumetric properties as a function of temperature at 0.1 MPa. *J. Chem. Eng. Data* **2008**, *53*, 716–726.
- (4) Bakis, E.; van den Bruinhorst, A.; Pison, L.; Palazzo, I.; Chang, T.; Kjellberg, M.; Weber, C. C.; Costa Gomes, M.; Welton, T. Mixing divalent ionic liquids: effects of charge and side-chains. *Phys. Chem. Chem. Phys.* **2021**, *23*, 4624–4635.
- (5) Jadhav, A. H.; Chinnappan, A.; Patil, R. H.; Kostjuk, S. V.; Kim, H. Short oligo ethylene glycolic tailor-made ionic liquids as highly efficient and reusable catalyst for one-pot synthesis of 1,5-benzodiazepine derivatives under solvent free condition. *Chem. Eng. J.* **2014**, *240*, 228–234.
- (6) Besnard, M.; Cabaço, M. I.; Vaca Chávez, F.; Pinaud, N.; Sebastião, P. J.; Coutinho, J. A.; Mascetti, J.; Danten, Y. CO₂ in 1-butyl-3-methylimidazolium acetate. 2. NMR investigation of chemical reactions. *J. Phys. Chem. A* **2012**, *116*, 4890–4901.
- (7) Zhang, Y.; Wu, Z.; Chen, S.; Yu, P.; Luo, Y. CO₂ Capture by Imidazolate-Based Ionic Liquids: Effect of Functionalized Cation and Dication. *Ind. Eng. Chem. Res.* **2013**, *52*, 6069–6075.